SPE 26436

Enhanced Reservoir Description: Using Core and Log Data to Identify Hydraulic (Flow) Units and Predict Permeability in Uncored Intervals/Wells

Jude O. Amaefule* and Mehmet Altunbay*, Core Laboratories; Djebbar Tiab*, U. of Oklahoma; David G. Kersey and Dare K. Keelan*, Core Laboratories

*SPE Member

Ω

Abstract

Understanding complex variations in pore geometry within different lithofacies is the key to improved reservoir description and exploitation. Core data provide information on various depositional and diagenetic controls on pore geometry. Variations in pore geometrical attributes in turn, define the existence of distinct zones (hydraulic units) with similar fluid-flow characteristics. Classic discrimination of rock types has been based on subjective geological observations and on empirical relationships between the log of permeability versus porosity. However, for any porosity within a given rock type, permeability can vary by several orders of magnitude, which indicates the existence of several flow units.

In this paper, a new, practical and theoretically correct methodology is proposed for identification and characterization of hydraulic units within mappable geological units (facies). The technique is based on a modified Kozeny-Carmen equation and the concept of mean hydraulic radius. The equation indicates that for any hydraulic unit, a log-log plot of a "Reservoir Quality Index," (RQI), which is equal to $0.0314\sqrt{k/\phi}$, versus a "Normalized Porosity Index" (ϕ_z) which is equal to $\phi/(1-\phi)$ should yield a straight line with a unit slope. The intercept of the unit slope line with $\phi_z = 1$, designated as the "Flow Zone Indicator" (FZI), is a unique parameter for each hydraulic unit. RQI, ϕ_z and FZI are based on stressed porosity and permeability data measured on core samples.

FZI is then correlated to certain combinations of logging tool responses to develop regression models for permeability predictions in cored and uncored intervals or wells. The proposed technique has been successfully tested in clastic rocks from East Texas, South America, West Africa, South East Asia and Far East Asia, as well as carbonate sequences from West Texas and Canada. This paper documents the theoretical development, validates and characterizes the hydraulic units, and presents predicted versus actual permeability data to demonstrate the efficacy of the proposed technique.

Introduction

One of the most important existing and emerging challenges of geoscientists and engineers is to improve reservoir description techniques. It is well recognized that improvements in reservoir description will reduce the amount of hydrocarbon left behind pipe. Accurate determination of pore-body/throat attributes and fluid distribution are central elements in improved reservoir description. Many reservoir description programs, though detailed, have not included descriptions at the pore-throat scale. Yet, pore-throat attributes control initial/residual hydrocarbon distribution and fluid flow. Because they are readily available, continuous sources of data, logging tool responses are often used to draw inferences about lithology, depositional and diagenetic sequences, and fluid content. These inferences are based on empirical models utilizing correlations among tool responses, rock and fluid properties. In many instances, unfortunately, the correlation models can not be used globally because of the influences of factors not fully considered by the models. Factors include (a) the presence of potassium-feldspar, zircon, etc. causing erroneously high calculated V_{sh} from the gamma ray; (b) microporosity in kaolinite, chert, etc. leading to high apparent water saturation calculations; and (c) siderite, pyrite, barite, and smectite influencing the resistivity, density and neutron log

205

calculations. The key to enhanced reserves determination and improved productivity is not based on the use of empirical correlations. It is based on the establishment of causal relationships among core-derived, microscopic pore-throat parameters and log-derived macroscopic attributes. These theoretically correct relationships can then be used as input variables to calibrate logs for improved reservoir description.

In this paper, a new, practical and theoretically sound methodology is introduced to identify and characterize hydraulic units within mappable geologic units (facies). This methodology uses core data to develop an understanding of the complex variations in pore geometry within different lithofacies. Core data provide information for various depositional and diagenetic controls on pore geometry. Variations in pore geometrical attributes, in turn, define the existence of distinct zones (hydraulic units) with similar fluid-flow characteristics. A hydraulic (pore geometrical) unit is defined as the representative elementary volume[1] (REV) "of total reservoir rock within which geological and petrophysical properties that affect fluid flow are internally consistent and predictably different from properties of other rock volumes."[2]

Hydraulic units are related to geologic facies distribution, but do not necessarily coincide with facies boundaries.[3] Therefore, hydraulic units may not be vertically contiguous. Hydraulic units are often defined by (a) geological attributes of texture, mineralogy, sedimentary structures, bedding contacts and nature of permeability barriers and by (b) petrophysical properties of porosity, permeability and capillary pressure.

Statement of the Problem

Classical Permeability-Porosity Relationships

Knowledge of permeability and permeability distribution is critical to effective reservoir description. Several authors[4,5,6] have noted the importance of these parameters for planning and implementation of completion strategies for successful waterflooding programs and for construction of representative simulation models for effective reservoir management. Permeability and permeability distribution are usually determined from core data. However, most wells are often not cored. As a result, permeability is estimated in uncored sections/wells from permeability versus porosity relationships that are often developed from statistically insignificant data sets. In uncored wells or zones, empirical permeability is estimated from log-derived porosity using Eq. 1.

$$\log k = a\phi + b \quad \dots \dots \dots \dots \dots \dots \dots \dots \dots \dots \dots (1)$$

There is apparently no theoretical basis to support the traditional crossplot of the logarithm of permeability versus porosity. Permeability is plotted as a log function only because it appears to be log-normally distributed. However, correlation of two normally distributed parameters does not necessarily establish causality. On the classical plot, the relationship between permeability and porosity is not causal. Whereas porosity is generally independent of grain size, permeability is strongly dependent on grain size. For example, in a reservoir, porosity and permeability may, in general, be directly proportional. Yet, in the same reservoir, there may be both high and low permeability zones with equal porosity values (Fig. 1). Therefore this traditional plot can not be used reliably to estimate accurate permeability from porosity data. Several investigators[5,7,8,9,10] have noted the inadequacy of this classical approach and have proposed alternative models for relating porosity to permeability. From the classical approach it can be concluded that for any given rock type, the different porosity/permeability relationships are evidence of the existence of different hydraulic units. Apparently several investigators[3,5,11] had come to a similar conclusion about porosity/permeability relationships.

In this paper, a theoretically correct, and fundamentally derived relationship between porosity and permeability is proposed. The influence of various geological (depositional and diagenetic) variables that control fluid flow are reflected in the proposed methodology.

Fundamental Theory

The hydraulic quality of a rock is controlled by pore geometry. This, in turn, is a function of mineralogy (i.e., type, abundance, morphology and location relative to pore throats) and texture (i.e., grain size, grain shape, sorting, and packing). Various permutations of these geological attributes often indicate the existence of distinct rock units with similar pore throat attributes. Determination of these pore throat attributes is central to accurate zoning of reservoirs into units with similar hydraulic properties. The mean hydraulic unit radius (r_{mh}) concept[12] is the key to unraveling the hydraulic units and relating porosity, permeability and capillary pressure.

$$r_{mh} = \frac{\text{Cross Sectional Area}}{\text{Wetted Perimeter}} = \frac{\text{Volume Open to Flow}}{\text{Wetted Surface Area}} \quad \dots (2)$$

For a circular, cylindrical capillary tube,

$$r_{mh} = \frac{r}{2} \quad \dots \dots \dots \dots \dots \dots \dots \dots \dots \dots \dots \dots \dots \dots \dots \dots (3)$$

By invoking the concept of the mean hydraulic radius, Kozeny[13] and Carmen[14] considered the reservoir rock to be composed of a bundle of capillary tubes. They then applied Poisseuille's and Darcy's Laws to derive a relationship (Eq. 4) between porosity and permeability. The primary assumptions in their derivation are that "the travel time of a fluid element in a capillary tube is equal to that in a REV,"[15] and that porosity is effective.

$$k = \frac{\phi_e r^2}{8\tau^2} = \frac{\phi_e}{2\tau^2}\left(\frac{r}{2}\right)^2 = \frac{\phi_e r_{mh}^2}{2\tau^2} \quad \dots\dots\dots\dots\dots (4)$$

The mean hydraulic radius (r_{mh}) can be related to the surface area per unit grain volume (S_{gv}) and effective porosity (ϕ_e) as follows:

$$S_{gv} = \frac{2}{r}\left(\frac{\phi_e}{1-\phi_e}\right) = \frac{1}{r_{mh}}\left(\frac{\phi_e}{1-\phi_e}\right) \quad \dots\dots\dots\dots (5)$$

Substituting Eq. 5 for r_{mh} in Eq. 4, Kozeny and Carmen obtained the following relationship

$$k = \frac{\phi_e^3}{(1-\phi_e)^2}\left[\frac{1}{2\tau^2 S_{gv}^2}\right], \quad \dots\dots\dots\dots\dots\dots (6)$$

where k is in μm^2 and ϕ_e is a fraction.

The generalized form of the Kozeny-Carmen relationship is given by Eq. 7.

$$k = \frac{\phi_e^3}{(1-\phi_e)^2}\left[\frac{1}{F_s\tau^2 S_{gv}^2}\right] \quad \dots\dots\dots\dots\dots (7)$$

where F_s is the shape factor (2 is for a circular cylinder). The term $F_s\tau^2$ has classically been referred to as the Kozeny constant. For ideal, uniform, and unconsolidated rocks, Carmen[14] and Leverett[16] computed the value of this term to be about 5. However, Rose and Bruce[17] showed that this term ($F_s\tau^2$) could vary from 5 to 100 in real reservoir rocks.

Many investigators[2-11] have attempted to calculate permeability from porosity by using Eq. 7. These attempts generally have not been successful due to the use of a constant value (typically 5) for $F_s\tau^2$ and the lack of consideration of S_{gv}^2 in these computations. In reality, the Kozeny constant is a variable "constant," which varies between hydraulic units, but is constant within a given unit.

The issue of the variability of the Kozeny constant is addressed in the following manner. Dividing both sides of Eq. 7 by porosity (ϕ_e) and taking the square root of both sides results in

$$\sqrt{\frac{k}{\phi_e}} = \left[\frac{\phi_e}{1-\phi_e}\right]\left[\frac{1}{\sqrt{F_s}\tau S_{gv}}\right] \quad \dots\dots\dots\dots (8)$$

where k is in μm^2.

However, if permeability is presented in millidarcies, then the following parameter can be defined:

$RQI\,(\mu m)$ = Resevoir Quality Index

$$= 0.0314\sqrt{\frac{k}{\phi_e}} \quad \dots\dots\dots\dots\dots (9)$$

ϕ_z is defined as the pore volume-to-grain volume ratio.

$$\phi_z = \left(\frac{\phi_e}{1-\phi_e}\right) \quad \dots\dots\dots\dots\dots\dots\dots (10)$$

FZI (μm), designated as the Flow Zone Indicator, is given by

$$FZI = \frac{1}{\sqrt{F_s}\tau S_{gv}} = \frac{RQI}{\phi_z} \quad \dots\dots\dots\dots (11)$$

Substituting these variables into Eq. 8 and taking the logarithm of both sides results in

$$\log RQI = \log\phi_z + \log FZI \quad \dots\dots\dots\dots (12)$$

On a log-log plot of RQI versus ϕ_z, *all samples with similar FZI values will lie on a straight line with unit slope.* Samples with different FZI values will lie on other parallel lines. The value of the FZI constant can be determined from the intercept of the unit-slope straight line at $\phi_z = 1$. *Samples that lie on the same straight line have similar pore throat attributes and, thereby, constitute a hydraulic unit.*

Alternative relationships that yield FZI values similar to those derived from Eq. 12 have also been developed from Eq. 7 as follows.

If k (md), FZI (μm) and ϕ_e (fraction), then

$$k = 1014\,(FZI)^2\left(\frac{\phi_e^3}{(1-\phi_e)^2}\right) \quad \dots\dots\dots\dots (13)$$

If ϕ_R is defined as

$$\phi_R = \frac{\phi_e^3}{(1-\phi_e)^2}, \quad \dots\dots\dots\dots\dots\dots (14)$$

then

$$k = 1014\,(FZI^2)\,\phi_R \quad \dots\dots\dots\dots\dots\dots (15)$$

Taking the logarithm of both sides of Eq. 15 then results in

$$\log k = \log(\phi_R) + \log[1014\,(FZI^2)]. \quad \dots\dots\dots (16)$$

A log-log plot of k versus ϕ_R results in a straight line with a unit slope and an intercept (at $\phi_R = 1$) of 1014 $(FZI)^2$.

Some investigators[6,18] have attempted to zone the reservoir into different layers by using the parameter (k/ϕ). Dividing both sides of Eq. 13 by ϕ results in

$$\frac{k}{\phi_e} = 1014\,(FZI)^2\left(\frac{\phi_e}{1-\phi_e}\right)^2 = 1014\,(FZI)^2\,(\phi_z)^2. \quad (17)$$

Taking the logarithm of both sides of Eq. 17 yields

$$\log\left(\frac{k}{\phi_e}\right) = 2\log\phi_z + \log[1014\,(FZI)^2]. \quad \dots\dots\dots (18)$$

A log-log plot of (k/ϕ) versus ϕ_z results in a straight line with a slope of 2 and an intercept of $\phi_z = 1$ of 1014 $(FZI)^2$. As noted earlier, all samples with similar FZI values belong to the same hydraulic unit and will, therefore, lie on the same straight line.

Geological Significance of FZI

Statistical techniques based only on variations in permeability have been used by previous investigators[19] to zone the reservoir into layers. The problem is that these approaches ignored geological attributes that control reservoir zonation.[20]

The Flow Zone Indicator (FZI) is a unique parameter that incorporates the geological attributes of texture and mineralogy in the discrimination of distinct pore geometrical facies (hydraulic units).

Data[21] displayed on Figs. 2 and 3 demonstrate the excellent correlation between S_{wr} (from capillary pressure), surface area (from NMR), weight percent of grains with sizes less than 30 microns (from wet sieve), and FZI. As expected, S_{wr} decreased with increasing FZI (Fig. 2). The relationship between S_{wr} and FZI can be represented mathematically by the following expression.

$$S_{wr} = 1 - \left[\frac{1}{a + bFZI^{-c}}\right], \qquad \ldots (19)$$

where $a = 1.12$, $b = 0.5634$, $c = 1.44$, and $r^2 = 0.998$. The relationship between S_{gv}, W (weight percent grains less than 30 microns) and FZI can be represented by the following equation:

$$Y = Y_{min} + (Y_{max} - Y_{min})\frac{X_{min}}{FZI} \qquad \ldots (20)$$

Values of Y_{min}, Y_{max}, and X_{min} are summarized in Table 1.

In general, rocks containing authigenic pore lining, pore filling, and pore bridging clays as well as fine grained, poorly sorted sands tend to exhibit high surface area and high tortuosity, hence low FZI (Table 3). In contrast, clean, coarse grained and well sorted sands exhibit lower surface areas, lower shape factor, lower tortuosity, and higher FZI values. In a related fashion, different depositional environments and diagenetic processes control pore geometry and FZI in carbonate rocks.

Hydraulic Unit Zonation Process

A detailed flowchart of the hydraulic unitization process is shown in Fig. 4. This process involves the application of classical statistical techniques including histogram/frequency diagrams, normality tests, cluster analysis, and error analysis for discriminating the hydraulic units. A one-dimensional FZI frequency histogram coupled with a classical test for normal distribution were used to discriminate the distinct family of hydraulic units. As documented by standard statistical textbooks,[22] intrinsic and unimodally distributed variables within

any given homogeneous population are approximately normally distributed. A probability plot of a unimodally and normally distributed variable often results in a straight line. In contrast, the existence of multiple, homogeneous subgroups within a given population often give rise to multimodal distributions and thus results in multiple straight lines on a probability plot.[22] Determination of the specific number of hydraulic units is constrained by random errors in the porosity and permeability data used to compute FZI. The magnitude of the random errors can be estimated by the root mean square technique.[23] Relative random errors in FZI computed from Eq. 21 were used to establish the uncertainty envelopes around FZI trend lines. All samples with the coefficient of variance $(\Delta FZI/FZI > 0.5)$ were considered unreliable and therefore were not used in the hydraulic unit zonation process. The following parameters were used to compute $(\Delta FZI/FZI)$ in Eq. 21: $(\Delta k/k = 0.2$; $\Delta\phi_e = 0.5\%$ (if ϕ_t is used instead of ϕ_e, then $\Delta\phi = 1\%$)).

$$\left(\frac{\Delta FZI}{FZI}\right) = \pm 0.5\left[\left(\frac{\Delta\phi}{\phi}\right)^2 \bullet \left(\frac{3-\phi}{1-\phi}\right)^2 + \left(\frac{\Delta k}{k}\right)^2\right]^{0.5} \ldots (21)$$

Validation and Characterization of Hydraulic Units: Case Histories

Confirmation of the validity of the proposed FZI technique for identification of distinct pore geometrical (hydraulic) units is provided by using a combination of the following technologies:

- Mineralogical and textural characteristics of each unit as determined from petrographic data (XRD, FTIR mineralogy, thin-section photography and SEM)

- RQI stress sensitivity

- Pore throat characterization as determined from mercury injection and/or centrifuge capillary pressure.

The size distribution of pore throat radii, determined from capillary pressure data, provides an independent method to corroborate the hydraulic unit zonation. The ratio of macro (r > 1.5 μm) plus meso (0.5μm < r < 1.5μm) to micro (r < 0.5 μm) is an excellent delineator of hydraulic units.

Manipulation of Eqs. 3-7 yields the fundamental relationship between FZI and the mean hydraulic radius (r_{mh}):

$$\log (r_{mh}) = \log (FZI) + \log (\sqrt{F_s}\tau\phi_z) \qquad \ldots (22)$$

Thus,

$$Y = mX, \qquad \ldots (23)$$

where $X = FZI$, $Y = \dfrac{r_{mh}}{\phi_z}$, and m = slope $= \sqrt{F_s}\tau$.

Fig. 5 provides the corroborative evidence of the soundness of the fundamental theory as depicted by the straight line in the center of the plot of r_{mh}/ϕ_z versus FZI. The slope is the product of $\sqrt{F_s}\tau$, which is equal to 6.74.

Four typical examples from clastic sequences in Texas, South America, South East Asia, and West Africa as well as two carbonate rock examples from West Texas and Canada are presented to demonstrate the worldwide applicability of this proposed technique.

Field Examples of Clastic Reservoirs

Travis Peak Formation, East Texas

The first step in the verification of this hydraulic unit zonation method is to compare the crossplot of the log of permeability versus porosity (Fig. 1). The log of permeability/porosity crossplot shows wide dispersion around the regression line (e.g., permeability varies up to four orders of magnitude for a given porosity). The dispersion is decreased when depositional environments are superimposed onto the plot. Samples deposited in the fluvial environment (lower interval) have higher permeability values for given porosities than samples deposited in the delta plain environment (Fig. 1). Replacement of the general regression line with regression lines for the upper and lower intervals reduces the dispersion.

Plotting the distribution of the major diagenetic clays highlights the impact of diagenesis on reservoir properties. Regardless of the depositional environment, the highest permeability values are associated with kaolinite, intermediate permeability values correlate with chlorite, and the lowest permeability values correlate with illite.

A log-log plot of RQI versus ϕ_z for this data set (Fig. 6) shows the existence of six distinct hydraulic units within the cored interval. Each hydraulic unit is characterized by a different average FZI value. The influence of diagenesis has modified the original depositional parameters to give these multiple hydraulic units.

South America

Porosity and permeability data generated on a typical South American clastic reservoir rock were used to compute RQI, ϕ_z, and FZI. A log-log plot of RQI versus ϕ_z (Fig. 7) shows five distinct hydraulic units within the cored interval. These units were discriminated by the previously discussed statistical techniques with the theoretical unit slope constraint.

Additionally, Fig. 8 shows the classical log k versus ϕ plot after the zonation process. The permeability response equations were derived from Eq. 13. It is evident from this plot that permeability is a nonlinear function of porosity, texture and mineralogy. The differences between the hydraulic units was further verified by water-oil capillary pressure data and cation exchange capacity (CEC) per unit pore volume (Q_V). It is evident on Fig. 9 that Q_V decreased with increasing FZI, thus manifesting the effect of clay minerals on the rock's hydraulic quality.

South East Asia

Porosity-permeability data from a clastic sequence from South East Asia were subjected to the hydraulic unitization process. Fig. 10 shows the existence of distinct hydraulic units within the cored interval as determined from a log-log plot of RQI versus ϕ_z. The different curves depicted on this figure indicate the FZI average for each of the seven hydraulic units.

Thin section photomicrographs[24] of samples from the various units shown on Figs. 11 to 15 substantiate the effectiveness of the proposed zonation process. Notice the effect of texture and mineralogy on the pore geometrical quality of the different units. For instance, comparison of Figs. 11A and 11B show the textural and mineralogical similarity of hydraulic unit 1 taken from both shallow and deep play samples. In contrast, hydraulic unit 2 (Fig. 12) is typified by a very fine to fine grained texture and a much higher clay content (10%) than hydraulic unit 1 (5%). Hydraulic unit 3 (Fig. 13) from a deep play is characterized by a coarse siltstone to very fine grained sandstone with a total clay content of 21%, while hydraulic unit 4 (Fig. 14) is a medium grained siltstone with a higher clay content of 25%. The seventh (Fig. 15) and worst unit is a argillaceous siltstone with a total clay content of 34%.

West Africa

Fig. 16 shows the classical log k versus ϕ plot for a typical data set from the Niger Delta. Seven distinct hydraulic units were established within the cored interval by utilizing the proposed techniques. As previously observed, the permeability-porosity relationship in the Niger Delta is also nonlinear and predictable (Eq. 13). FZI ranged from 0.3 to well over 11 in these depositional/diagenetic sequences. The variability of FZI in the Niger Delta rocks appears to be both texturally and mineralogically controlled.

Fig. 17 documents the intrinsic pore geometrical characteristics and reflects the effect of geological attributes (Figs. 18A to 18C) on hydraulic quality. For example, hydraulic unit 4 (FZI = 4.83), which is a fine-grained, moderately well-rounded and well-sorted sand with a low clay content (1% kaolinite) (Fig. 18A), had the following distribution of pore throat sizes: macro = 83%, meso = 2%, and micro = 15%. In contrast, a sample from hydraulic unit 5 (FZI = 3.7), with a pore throat size distribution of macro = 68%, meso = 5%, and micro = 27%, is comprised of laminated, coarse and fine grained sequences with angular, poorly sorted grains and an intermediate clay content (5% kaolinite) (Fig. 18B). The worst quality hydraulic unit (FZI = 0.4), which is comprised of laminated, fine grained, well rounded, moderately sorted sandstone sequences, had a high clay content (12% kaolinite and chlorite) (Fig. 18C) and a pore throat size distribution of macro = 22, meso = 29, and micro = 49%.

Porosity and permeability data determined at multiple net overburden pressures were used to characterize the RQI stress sensitivity of each hydraulic unit. RQI was correlated to net overburden stress (σ) by the following relationship:[25]

$$Y = \frac{RQI}{RQI_i} = EXP\left[-b_s \bullet \left[1 - EXP\left(-\left(\frac{\sigma - \sigma_i}{c}\right)\right)\right]\right] \ldots (24)$$

where b_s = stress sensitivity factor, σ_i = initial stress used for RQI_i, and c = stress constant (2000-4000 psi).

The stress sensitivity factor (b_s) was further correlated to FZI, which was computed from porosity and permeability at initial stress conditions, to arrive at the following predictive relationship:

$$Y = b_s = A_1 - \left[\frac{B_1\left(\frac{x}{x_o} - 1\right)^{n_1}}{C_1\left(\frac{x}{x_o} - 1\right)^{n_1} + D}\right] \ldots \ldots \ldots \ldots (25)$$

For the Niger Delta clastic rocks, the RQI stress sensitivity (b_s) was correlated to FZI with the following parameters: $A_1 = 1.39$, $X = FZI$, $X_o = FZI_{min}$, $B_1 = 1.31$, $C_1 = 0.96$, $D_1 = 5.2$, $n_1 = 2.09$, with a coefficient of determination ($R^2 = .9999$). In general, it was established that rocks from the same hydraulic unit (similar FZI) exhibited similar RQI stress sensitivities (b_s). b_s decreased with increasing FZI. Additionally, rocks with abundant macropore throats typically showed lower RQI stress sensitivities ($b_s < 0.05$), in contrast to microporosity-dominated rocks that showed higher b_s values ($b_s > 0.05$).

The classical J function is not adequate for differentiating the various hydraulic units. This is because the J function only normalizes capillary pressure with respect to porosity, permeability and tortuosity, but does not include the effect of surface area. Eq. 26 confirms this observation.

$$J = \frac{P_c\sqrt{\frac{k}{\phi}}}{\sigma\cos\theta} = \frac{2}{r}\sqrt{\frac{k}{\phi}} = \frac{RQI}{r_{mh}} = \frac{1}{\sqrt{F_s}\tau} \ldots \ldots \ldots \ldots (26)$$

It is for this reason that no global J function appears plausible for normalization of capillary pressure.

Therefore, a more generalized water saturation versus capillary pressure model was developed based on the concept of the hydraulic unit. The proposed relationship (Eq. 27) is well behaved.

$$S_w = S_{wr} + (1 - S_{wr})e^{\left[-(FZI - FZI_{min})\left[S_{wr}ln\left(\frac{P_c}{P_d}\right)\right]\right]} \ldots (27)$$

As FZI tends to FZI_{min}, S_w approaches 1 as expected. Similarly, as $P_c = P_d$, S_w also approaches 1. However, as FZI or P_c approaches large values, S_w approaches the irreducible saturation S_{wr}. Fig. 19 shows a typical Niger Delta example on the application of the proposed model. This model has also been successfully applied to rocks from the UK North Sea and South East Asia.

Field Examples of Carbonate Reservoirs

Canada

Fig. 20 shows the distribution of FZI values versus class intervals for a Canadian carbonate rock. The existence of three distinct, uniformly distributed families of k versus ϕ (Fig. 21) are quite apparent on the classical crossplot with median FZI values of 1.5, 6.8, and 12.5. This example clearly demonstrates the applicability of this technique to all rock types.

West Texas

The crossplot of log permeability versus porosity shows the scatter common in many carbonate reservoirs (Fig. 22). Zoning the interval into hydraulic units shows six distinct FZI groups (Table 3). The grouping into six units is supported by independent geological and engineering data. In this example, petrology and mercury-injection capillary pressure were performed on selected samples from each hydraulic unit.

The effects of the depositional environment on pore throat attributes were examined. As expected in Paleozoic carbonate reservoirs, the overprint of diagenesis (Table 4) has significantly altered the original depositional pore/grain relationships. The slight correlation of mottling (i.e., bioturbation) with FZI shows the residual influence of the depositional environment on reservoir quality.

In comparison, diagenetic effects are directly related to FZI. An inverse correlation ($r^2 = 0.9999$) of dolomite/calcite with FZI results from the initial diagenetic development and subsequent partial dissolution of dolomite.

Pore-throat size distributions were calculated from the capillary pressure data. The ratio of macropore to micropore throat sizes is directly proportional to FZI.

Hydraulic Units and Permeability Prediction from Core and Log Data

A typical Far East Asia example was used to demonstrate the integration of core and log data to identify hydraulic units and to predict permeability. A flowchart of the process is shown on Fig. 23. Initially, the core depth was matched to the wireline log depth by comparing the total/spectral gamma derived from log and core data. Next the proposed zonation process was developed from stressed core (porosity and Klinkenberg permeability) data from the cored interval. Based on this process, six distinct hydraulic units were identified within the cored interval. The result of this zonation process is shown on the log k versus ϕ plot in Fig. 24. As expected, each pore geometrical family had similar average r_{mh} and FZI values.

Selection of the Wireline Data for the Derivation of Transform Equations

Environmentally corrected wireline log data were selected based on their ability to reflect the pore space attributes such as clays (type, abundance, location, morphology), pore-throat geometry and effective porosity. Individual wireline tool responses can not be directly correlated with the pore-space/throat attributes. Therefore, a statistical evaluation of the correlation between wireline data and pore-space/throat attributes is performed for each case. Selected log data are then used as variables in a transform equation to generate the permeability profiles.

A set of environmentally-corrected wireline logging tool responses (γ, $\phi_N-\phi_D$, ϕ_D, Δ_t, Rxo, R_t) were rank-correlated to FZI using Spearman's Rho Statistical Technique.[25]

Derivation of Regression Models for FZI and Permeability

A matrix of known core (FZI, RQI and k) values and corresponding wireline log responses is created for each hydraulic unit. A logarithmic filtering of the data is performed to normalize the data distribution by calculating the logarithm of each variable. Then, a matrix of the logarithms of normalized independent variables and logarithm of the normalized dependent variable (FZI, RQI or k) are generated. Quadratic, multilinear, or linear models[26] with modifications are then selected to form the basis for the transform equations. The transformation matrix is standardized by subtracting the mean of each column from the row variable itself and dividing the result by the standard deviation of that column.

Transform equations for each hydraulic unit were derived from the models and assigned to the corresponding depth points based on the hydraulic unit profile.

Qualitative Predictions of Hydraulic Units for the Uncored Sections

Qualitative predictions for the uncored sections of each well are performed by using a probabilistic method with a deterministic tool. The probabilistic method uses relationships implicit in the data to derive results. It does not require any assumption or predetermined equations. Results are obtained by statistical inferences. The deterministic tool that complements this methodology is the hydraulic unitization process that has been performed individually and independently on each well. Therefore, although it seems like a contradiction in terms, the deterministic approach (i.e., hydraulic units profile of the cored sections) enhances the reliability of the predictions of a probabilistic tool, because it provides a reliable and mathematically sound inference database. Probabilities are computed from estimated distributions of each hydraulic unit by application of the Bayes Theorem.[27] Level by level, transition matrices were created and solved to establish a vertical association between hydraulic units. Details of the probabilistic techniques are well documented.[27]

The discrimination matrix created from the control well(s) is used as a reference set (a set of histograms for every log for each hydraulic unit) for the neighboring uncored well(s) to determine the probability of having the same hydraulic unit in a given prediction window. This then forms the basis for the qualitative predictions of hydraulic units in an uncored well.

Fig. 25 shows the output of a case study using the proposed technique on a Far East Asia well in a typical logging trace with eight tracks. The hydraulic unit numbers starting from the best to the worst are assigned to the extreme right track (track 8). In the first well, the interval from X420 to X500 feet was cored. Data from X420-X472 were used to develop the hydraulic unit tracks and regression models from wireline logs. Hydraulic units were subsequently predicted for the section X472 to X500 and permeability determined from the regression models for those units. Without hydraulic unitization, permeability predicted from wireline logging tool response through the classical multilinear correlation technique shows significant deviations from actual measured values with $r^2 \approx .22$ (Fig. 26). In contrast, permeability predicted from the same logging tool responses after hydraulic zonation (Fig. 27) exhibits excellent correlations ($r^2 > .999$) with the actual measured values in the cored interval. Fig. 28 compares the permeability predicted from the classical log permeability vs. porosity crossplot to permeability derived from logging tool responses after hydraulic unitization using actual measured permeability values in another interval. As is evident on this plot, the classical log permeability versus porosity correlation underestimates permeability for k > 50 md in contrast to the proposed hydraulic unit controlled log-derived permeability.

In a second uncored well, the proposed process was used to predict the hydraulic unit profiles and to assign the regression equations for permeability determination based on logging parameters (Fig. 29). This hydraulic unit process also has been successfully applied in the Norwegian North Sea for permeability prediction.[28] More extensive theoretical developments dealing with clastic, carbonate and naturally fractured reservoirs can be found in Tiab.[29]

Conclusions

A new, practical and theoretically-based technique has been developed to identify and characterize units with similar pore throat geometrical attributes (hydraulic units). This technique has a wide variety of practical field applications for both cored and uncored wells. These include:

- Improved prediction of permeability and permeability distributions from wireline logs in partially cored/uncored intervals and adjacent wells

- Improved well-to-well rock properties correlations for refinement of petrophysical models

- Forecasts reservoir rock quality (and formation damage potential) in partially cored/uncored wells for improved completions and enhanced recovery decisions

- Provides a unique parameter, the Flow Zone Indicator (FZI) for delineating the number of layers (hydraulic units) required for assignment of geological and petrophysical parameters in numerical simulators.

The proposed hydraulic unit process has been successfully applied worldwide for both clastic (East Texas, South America, West Africa, South East Asia and Far East Asia) and carbonate (Canada and West Texas) rocks.

Nomenclature

b_s = stress sensitivity factor
c = critical stress constant (2000-4000 psi)
F_s = shape factor
$F_s \tau^2$ = Kozeny constant
k = permeability (μm^2)
r = pore throat radius (μm)
r_{mh} = mean hydraulic radius (μm)
RQI = Reservoir Quality Index (μm)
σ = overburden stress (psi)
σ_i = initial overburden stress (psi)
S_{gv} = surface area per unit grain volume (μm^{-1})
S_w = water saturation (fractional pore volume)
S_{wr} = irreducible water saturation (fractional pore volume)
ϕ_e = effective porosity (fraction bulk volume)
ϕ_R = reduced porosity index
ϕ_z = pore volume-to-grain volume ratio
τ = tortuosity

Acknowledgments

References

1. Bear, J.: *Dynamics of Fluids in Porous Media*, New York, Elsevier (1972).

2. Ebanks W.J., Jr.: "Integrated Approach to Reservoir Description for Engineering Projects," (abstract only) AAPG Abstract Flow Unit Concept.

3. Hearn, C.L., Ebanks, W.J., Tye, R.S. and Ranganathan, V.: "Geological Factors Influencing Reservoir Performance of the Hartzog Draw Field, Wyoming," JPT v. 36 No. 9 (August 1984) 1335-1344.

4. Shirer, J.A., Langston, E.P., and Strong, R.B.: "Application of Field-Wide Conventional Coring in the Jay-Little Escambia Creek Unit," *JPT* (December 1978) 1774-1780.

5. Stiles, J.H., Jr. and Hutfilz, J.M.: "The use of Routine and Special Core Analysis in Characterizing Brent Group Reservoirs, U.K. North Sea," SPE 18388 (1988).

6. Chopra, A.K., Stein, M.H. and Ader, J.C.: "Development of Reservoir Description to Aid in Design of EOR Project," SPE 16370, presented at the SPE California Regional meeting, Ventura, California (1987).

7. Dorfman, M.H., Newey, J.J., and Coates, G.R.: "New Techniques in Lithofacies Determination and Permeability Prediction in Carbonates using Well Logs" (1990) 113-120, in *Geological Applications of Wireline Logs*, A. Hurst, M.A. Lovell and A.C. Morton, Eds., Geological Society Special Publication No. 48.

8. Dubrule, O. and Haldorsen, H.H.: "Geostatistics for Permeability Estimation," *Reservoir Characterization*, L.W. Lake and H.B. Carroll, Jr. (eds.), Academic Press (1986) 223-247.

9. Timur, A.: "An Investigation of Permeability, Porosity and Residual Water Saturation Relationships," Trans. SPWLA Ninth Annual Logging Symposium (1968) Paper K.

10. Wendt, W.A., Sakurai, S. and Nelson, P.H.: "Permeability Prediction from Well Logs Using Multiple Regression," *Reservoir Characterization*, L.W. Lake and H.B. Carroll, Jr. (eds.), Academic Press (1986) 181-221.

11. Slatts, R.M. and Hopkins, G.L.: Scaling Geologic Reservoir Description to Engineering Needs," JPT, v. 42, No. 2 (February 1990) 202-211.

12. Bird, R.B., Steware, W.E. and Lightfoot, E.N.: *Transport Phenomena*, New York, Wiley (1960).

13. Kozeny, J.: "Uber Kapillare Leitung des Wassers im Boden, Sitzungsberichte," Royal Academy of Science, Vienna, Proc. Class I (1927) v. 136, 271-306.

14. Carmen, P.C.: "Fluid Flow through Granular Beds," Trans. AIChE (1937) v. 15, 150-166.

15. Lake, L.W.: *Enhanced Oil Recovery*, Prentice Hall, Englewood Cliffs, New Jersey (1989).

16. Leverett, M.C.: "Capillary Behavior in Porous Solids," Petroleum Technology, T. P. 1223 (1940) 152-169.

17. Rose, W. and Bruce, W.A.: "Evaluation of Capillary Character in Petroleum Reservoir Rock," Petroleum Transactions, AIME (1949) 127-142.

18. Chopra, A.K.: "Reservoir Descriptions Via Pulse," SPE 17568 Int'l Meeting on Petroleum Engineering, Tianjin, China (1988) 171-87.

19. Testerman, J.D.: "A Statistical Reservoir-Zonation Technique," JPT (August 1962) 889-893; *Trans.*, AIME.

20. Weber, K.J. and van Geuns, L.C.: "Framework for Constructing Clastic Reservoir Simulation Models," JPT v. 42 No. 10 (October, 1990) 1248-1253 and 1296-1297.

21. Zemanek, J.: "Low-Resistivity Hydrocarbon-Bearing Sand Reservoirs," SPE 15713, SPE Middle East Oil Show (1987) 185-97/SPEFE (Dec. 1989) 515-21.

22. Taylor, J.K.: *Statistical Techniques for Data Analysis*, Lewis Publishers, Inc., Michigan (1990).

23. Amaefule, J.O., and D.K. Keelan: "Stochastic Approach to Computation of Uncertainties in Petrophysical Properties," SCA Paper 8907 (1989) 1-28.

24. Barr, D.C. and Altunbay, M.: "Identifying Hydraulic Units as an Aid to Quantifying Depositional Environments and Diagenetic Facies," Geological Soc. of Malaysia Symp. on Reservoir Evaluation/Formation Damage, Kuala Lumpur (July 11, 1992).

25. Amaefule, J.O., D.G. Kersey, D.M. Marshall, J.D. Powell, L.E. Valencia and D.K. Keelan: "Reservoir Description: A Practical Synergistic Engineering and Geological Approach based on Analysis of Core Data," SPE 18167 (1988) 1-30.

26. Chaterjee, Samprit and Price, Bertram: *Regression Analysis by Example*, New York, NY, John Wiley and Sons (1977).

27. Tetzlaff, D.M., Rodriguez, E. and Anderson, R.L.: "Estimating Facies and Petrophysical Parameters from Integrated Well Data," Paper *, Log Analysis Software Evaluation and Review (LASER) Symp. Trans., Soc. of Well Log Analysts, London Chapter, London, England (Dec. 13-15, 1989).

28. Cooper, R.D. and Oliveira, A.M.B.: "The Integration of Core Permeability, Log-Derived Permeability and Measured Flow Profiles in the Study of Cut-Off Criteria," SPWLA Permeability Seminar (May 18, 1992).

29. Tiab, D.: "Modern Core Analysis Manuscript," Internal Core Laboratories publication (May, 1993).

Table 1. Relationship between Surface Area, Weight Percent Grains < 30μ and FZI[21]

Parameter	Surface Area (NMR)	Weight % (Wet Sieve)
Y	S_{gv}	W
Y_{max}	153.50 m^2/g	19.79%
Y_{min}	16.92 m^2/g	13.68
X_{min}	0.10 μm	0.80 μm
R^2	0.95	0.995

Table 2. Effects of Geological Attributes on Hydraulic Unit Variables

| Geologic Attribute	Qualitative Effects On					
	F_s	τ	S_{gv}	FZI	S_{WR}	r_{mh}
Texture						
Coarse grained	L	L	L	H	L	H
Fine grained	H	H	H	L	H	L
Coarse grained, well sorted	L	L	L	H	L	H
Coarse grained, poorly sorted	H	H	H	L	H	L
Fine grained, well sorted	M	M	M	M	M	M
Mineralogy						
High clay content - smectite /illite/chlorite	H	H	H	L	H	L
High clay - kaolinite	M	M	M	M	M	M
Low clay content at pore throat - smectite	H	H	H	L	H	L

L = Low
M = Medium
H = High

$$FZI = \frac{1}{\sqrt{F_s}\tau S_{gv}}$$

Table 3: Depositional Model for a West Texas Carbonate

HU	Depth (ft)	φ (%)	k (md)	RQI	FZI	Features
1	6436	7.9	21.87	0.522	6.090	faintly mottled; small anhydrite patches
2	6390	8.8	6.38	0.267	2.774	faintly mottled; small to large anhydrite patches; faintly to moderately laminated
3	6417	10.1	2.23	0.148	1.313	mottled to massive; small anhydrite patches; faint allochem ghosts
4	6491	10.4	1.43	0.116	1.005	massive to faintly laminated; bird's eye anhydrite; fine stylolites
5	6454	8.3	0.37	0.066	0.732	massive to faintly mottled; small anhydrite patches; common allochem ghosts
6	6621	19.4	0.76	0.062	0.258	massive to faintly mottled; small anhydrite patches; faint allochem ghosts; healed fractures

Table 4: Diagenetic Model for a West Texas Carbonate

HU	Depth (ft)	RQI	Cements	Crystal Size and Morphology	Pore Types	Other
1	6436	0.522	scattered sparry calcite small patches of anhydrite	fine-med. crystalline avg = 0.06 mm subhedral to euhedral	intercrystalline	
2	6390	0.267	large patches of anhydrite, some possibly vug filling	medium crystalline avg = 0.23 mm subhedral to euhedral	intercrystalline	
3	6417	0.148	patchy sparry calcite patchy anhydrite	finely crystalline avg = 0.04 mm anhedral to subhedral	intercrystalline microporosity	common allochem ghosts
4	6491	0.116	bird's eye anhydrite minor scattered sparry calcite	finely crystalline avg = 0.05 mm anhedral to subhedral	intercrystalline possible pin-point vugs	allochem molds
5	6454	0.066	minor scattered calcite & anhydrite	bimodal crystalline size: very finely and medium crystalline avg = 0.007 and 0.014 mm anhedral to subhedral	intercrystalline moldic microporosity	common dolomite-replaced allochems allochem molds
6	6621	0.062	anhydrite-healed fractures minor sparry calcite	very finely to finely crystalline avg = 0.013 mm anhedral; minor euhedral	intercrystalline microporosity	allochem molds minor allochem ghosts
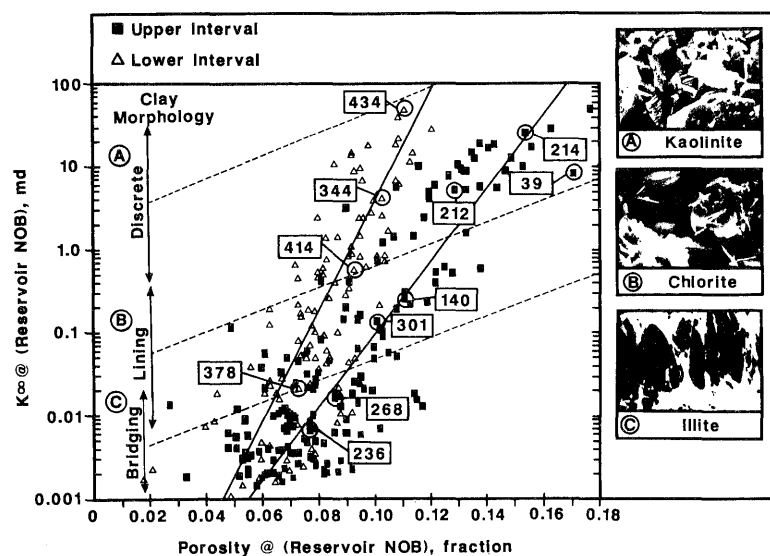
Fig. 1.   Plot of log permeability versus porosity (upper and lower intervals), East Texas example.[25]
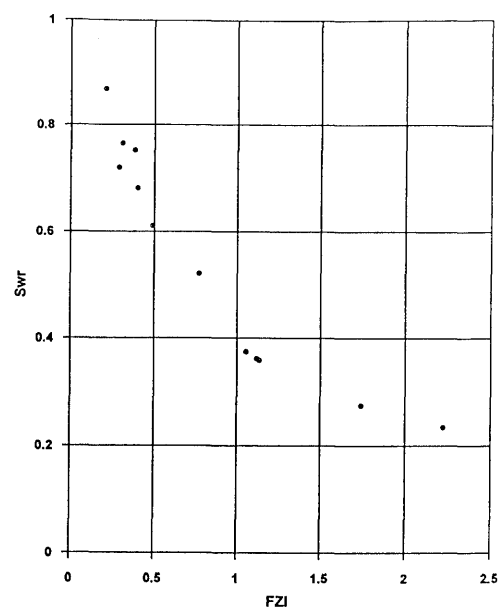
Fig. 2. S_{wr} (Capillary Pressure) versus FZI.[21]
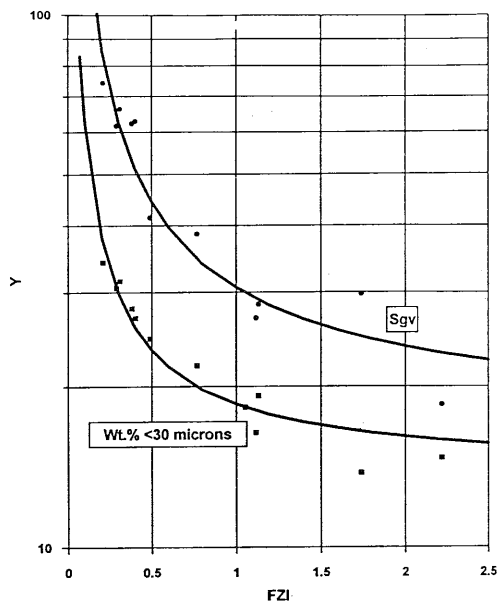
Fig. 3.   Surface area per unit grain volume (S_{gv}) and weight percent grains < 30 microns versus FZI.[21]
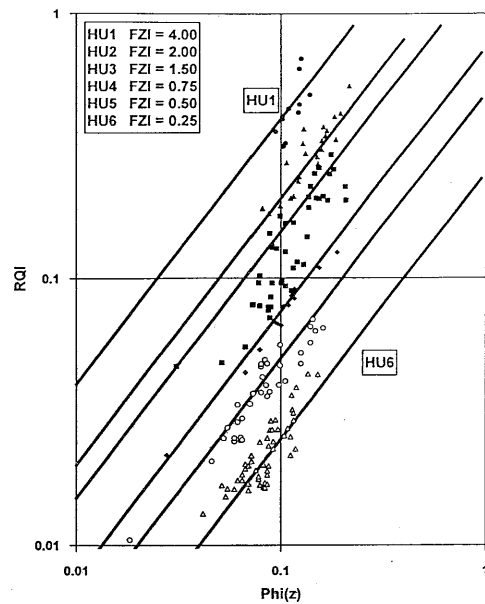
Fig. 6.   Plot of log RQI versus log ϕ_z for East Texas.
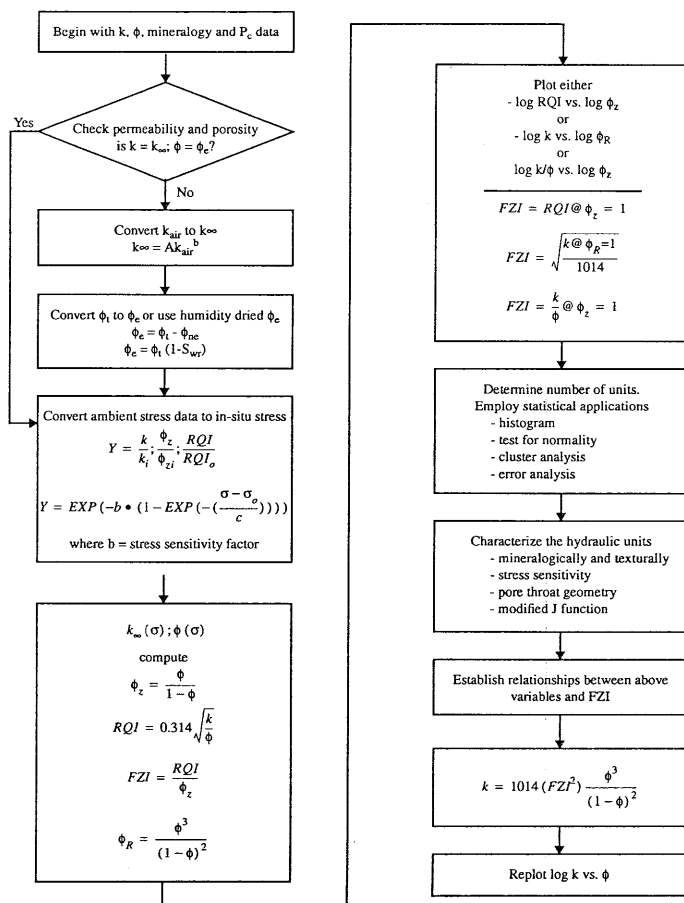
Fig. 4. Flowchart for characterization of hydraulic units.

Begin with k, ϕ, mineralogy and P_c data

Check permeability and porosity is $k = k_\infty$; $\phi = \phi_e$? — Yes / No

Convert k_{air} to k_∞
$$k_\infty = A k_{air}^b$$

Convert ϕ_t to ϕ_e or use humidity dried ϕ_e
$$\phi_e = \phi_t - \phi_{ne}$$
$$\phi_e = \phi_t (1 - S_{wr})$$

Convert ambient stress data to in-situ stress
$$Y = \frac{k}{k_i}; \frac{\phi_z}{\phi_{zi}}; \frac{RQI}{RQI_o}$$
$$Y = EXP(-b \bullet (1 - EXP(-(\frac{\sigma - \sigma_o}{c}))))$$
where b = stress sensitivity factor

$k_\infty(\sigma); \phi(\sigma)$
compute
$$\phi_z = \frac{\phi}{1 - \phi}$$
$$RQI = 0.314 \sqrt{\frac{k}{\phi}}$$
$$FZI = \frac{RQI}{\phi_z}$$
$$\phi_R = \frac{\phi^3}{(1 - \phi)^2}$$

Plot either
- log RQI vs. log ϕ_z
or
- log k vs. log ϕ_R
or
log k/ϕ vs. log ϕ_z

$$FZI = RQI @ \phi_z = 1$$
$$FZI = \sqrt{\frac{k @ \phi_R = 1}{1014}}$$
$$FZI = \frac{k}{\phi} @ \phi_z = 1$$

Determine number of units.
Employ statistical applications
- histogram
- test for normality
- cluster analysis
- error analysis

Characterize the hydraulic units
- mineralogically and texturally
- stress sensitivity
- pore throat geometry
- modified J function

Establish relationships between above variables and FZI

$$k = 1014 (FZI^2) \frac{\phi^3}{(1 - \phi)^2}$$

Replot log k vs. ϕ

Fig. 5.   Plot of r_{mh}/ϕ_z versus FZI.

Fig. 7.   Crossplot of log RQI versus log ϕ_z (South American example).

HU1 FZI = 7.63
HU2 FZI = 5.08
HU3 FZI = 3.62
HU4 FZI = 1.43
HU5 FZI = 0.14

Classical relationship: k(md) = 0.0033*3.6E17^Phi

HU-k relationship: k(md) = 1014*(FZI^2)*(Phi^3/(1-Phi)^2)
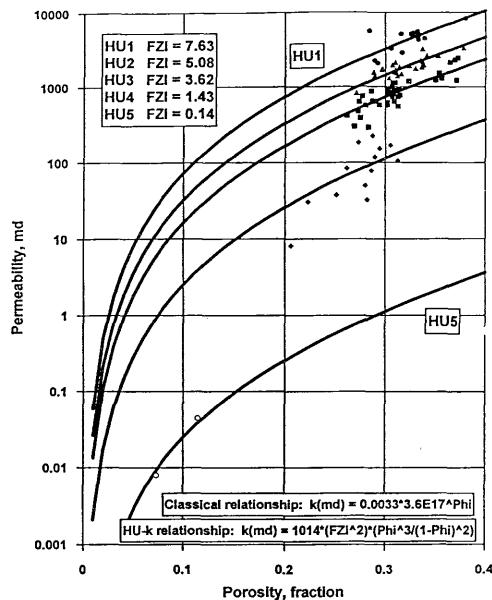
Fig. 8.   Crossplot of permeability versus
porosity for different hydraulic units
(South American example).
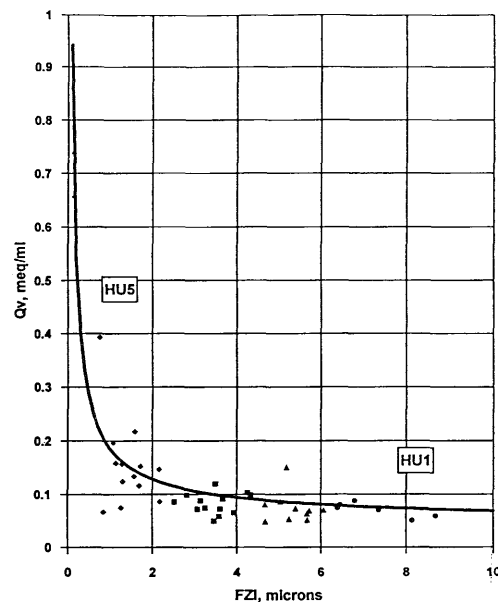
Fig. 9.   Cation exchange capacity (Q_v) versus
FZI (South American example).

HU1 FZI = 7.57
HU2 FZI = 4.42
HU3 FZI = 2.31
HU4 FZI = 1.04
HU5 FZI = 0.57
HU6 FZI = 0.29
HU7 FZI = 0.11
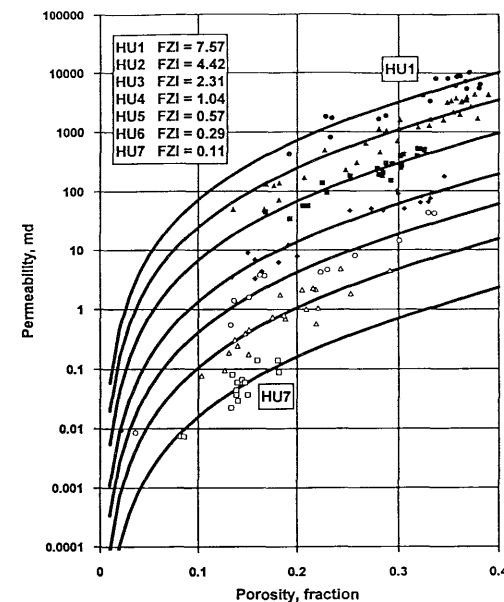
Fig. 10.   Crossplot of permeability versus
porosity for different hydraulic units
(South East Asian example).
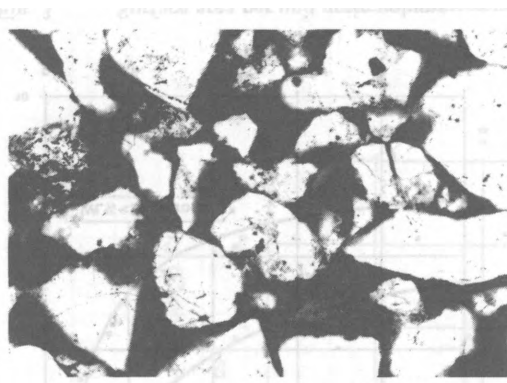
Fig. 11A.   Hydraulic Unit #1 (Shallow Play), Fine
to medium grained sandstone. $\phi =$
29.9%, k = 712md
Total Clay = 5.0%
(South East Asian example)
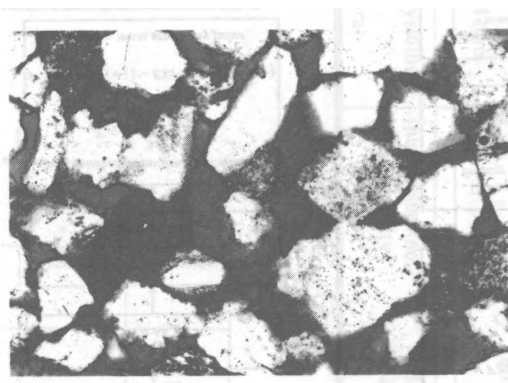
Fig. 11B.   Hydraulic Unit #1 (Deep Play), Fine to
medium grained sandstone. $\phi = 28.9\%$,
k = 813md
Total Clay = 6.4%
(South East Asian example)

Fig. 12.   Hydraulic Unit #2 (Shallow Plan), Very
fine to fine grained sandstone. $\phi =$
29.0%, k = 308md
Total Clay = 10.0%
(South East Asian example)
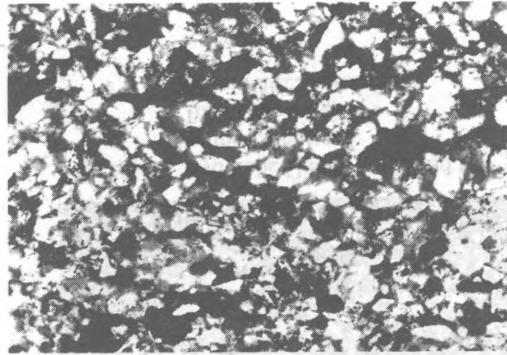
Fig. 13. Hydraulic Unit #3 (Deep Play), Coarse siltstone to vary fine grained sandstone.
φ = 29.4%, k = 60md
Total Clay = 21.0%
(South East Asian example)
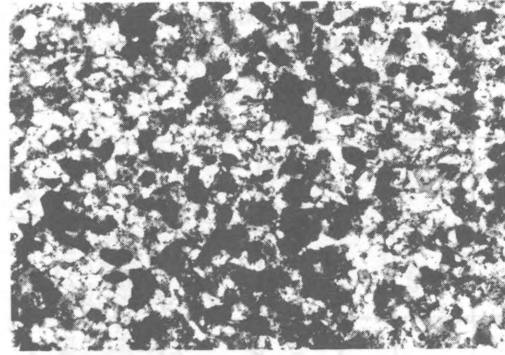
Fig. 14. Hydraulic Unit #4 (Deep Play), Medium grained siltstone.
φ = 27.2%, k = 10.2md
Total Clay = 25.0%
(South East Asian example)
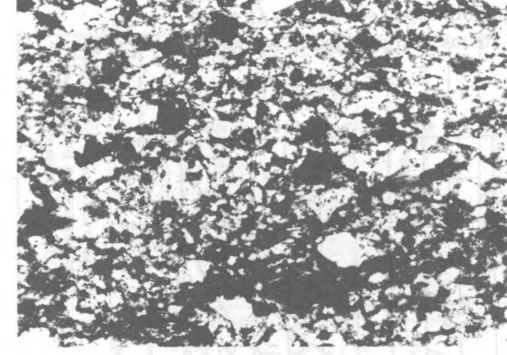
Fig. 15. Hydraulic Unit #7 (Deep Play), Very argillaceous siltstone. φ = 9.9%, k = 0.001md
Total Clay = 34.0%
(South East Asian example)
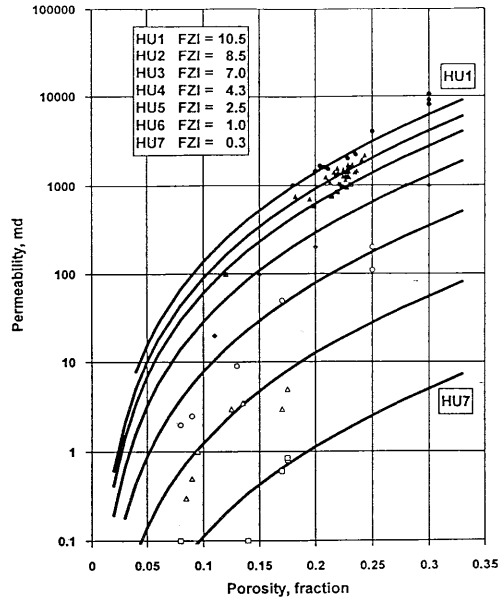
Fig. 16. Crossplot of Klinkenberg permeability versus porosity (West African example).
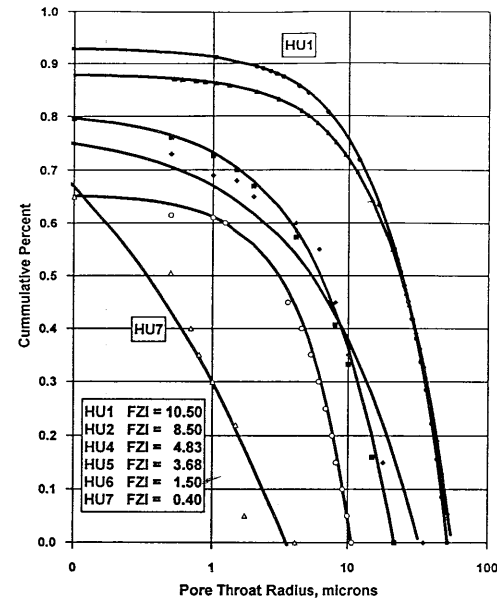
Fig. 17. Average pore throat size distribution for various hydraulic units (West African example).

Fig. 18A.   Hydraulic Unit 4, fine grained sandstone.
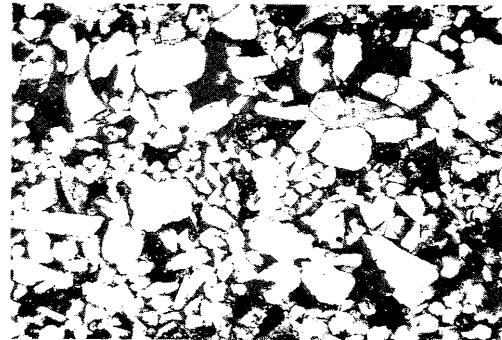Total Clay = 1%
(West African example)

Fig. 18B.   Hydraulic Unit 5, laminated fine and coarse grained sandstone.
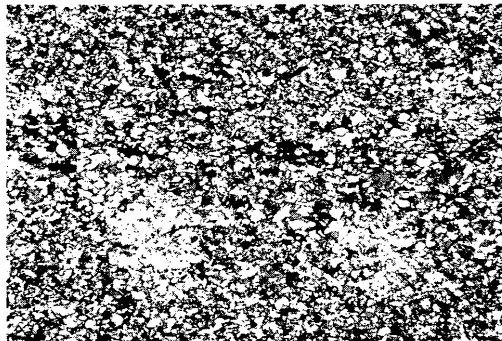Total Clay = 5%
(West African example)

Fig. 18C.   Hydraulic Unit 6, laminated fine grained sandstone.
Total Clay = 12%
(West African example)

Fig. 19. S_w versus normalized capillary pressure fraction (Pc/Pd) (West African example).

Fig. 20.   FZI versus class interval (Canadian example).

Fig. 21.   Crossplot of permeability versus porosity (Canadian example).

Fig. 22.   Crossplot of permeability versus porosity for various hydraulic units (West Texas example).
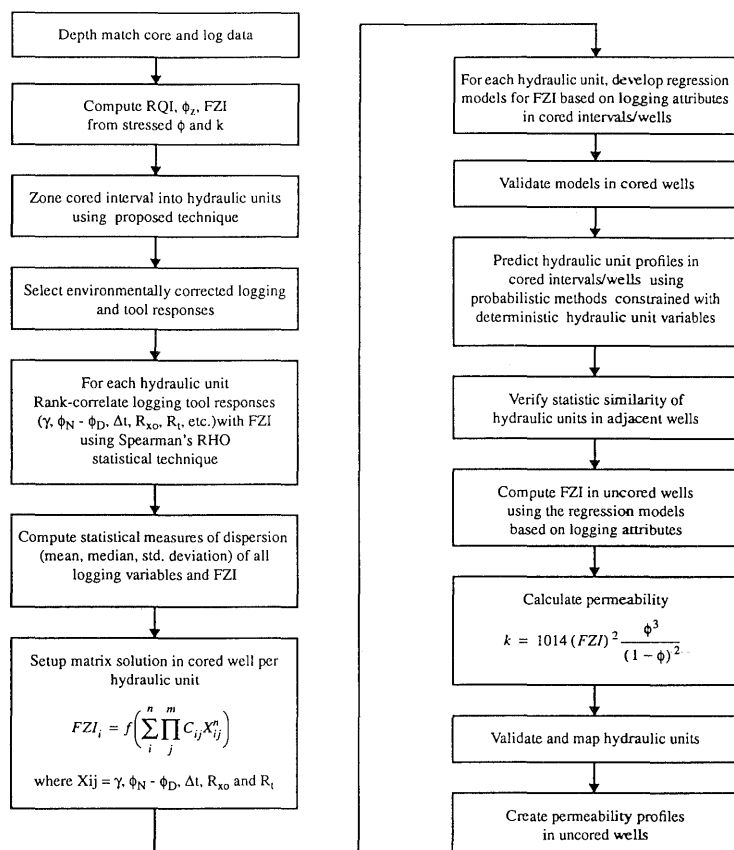
Fig. 23.   Prediction of hydraulic units and permeability from core and log data.
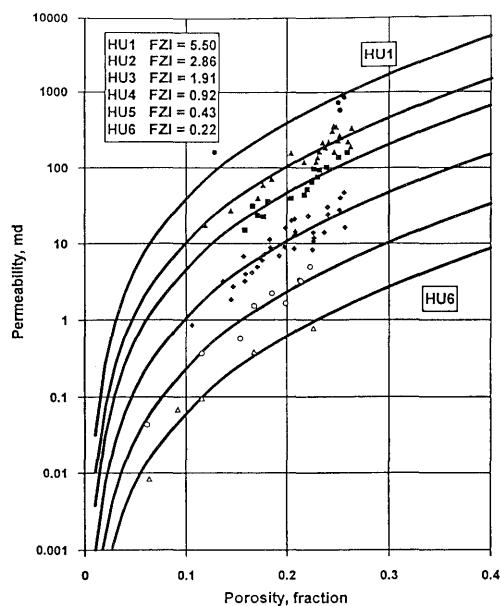
Fig. 24.   Crossplot of permeability versus porosity for various hydraulic units (Far Eastern example).
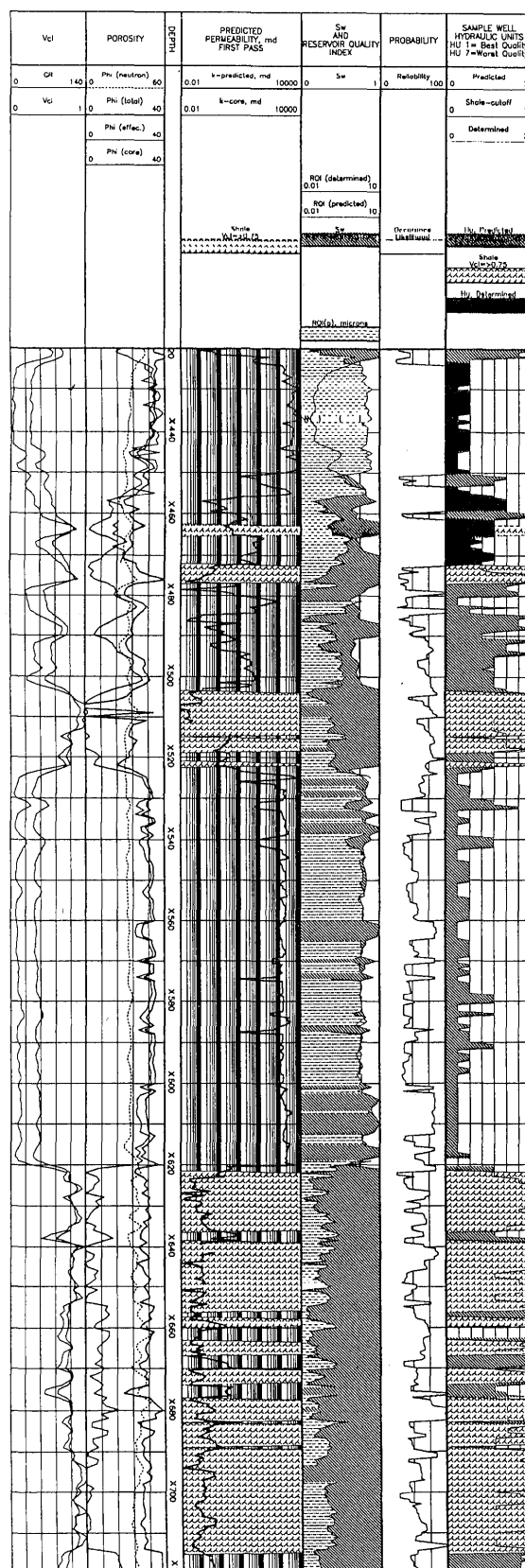
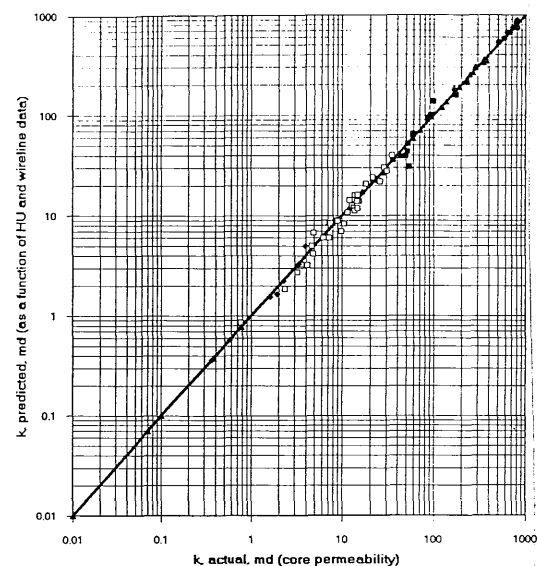Fig. 25.   Permeability profile predicted from logging in a cored interval (Far Eastern Example).

Fig. 26.   Predicted permeability versus core
            permeability without hydraulic
            unitization (Far Eastern example).

Fig. 27.   Predicted permeability with hydraulic
            unitization versus core permeability
            (Far Eastern example).
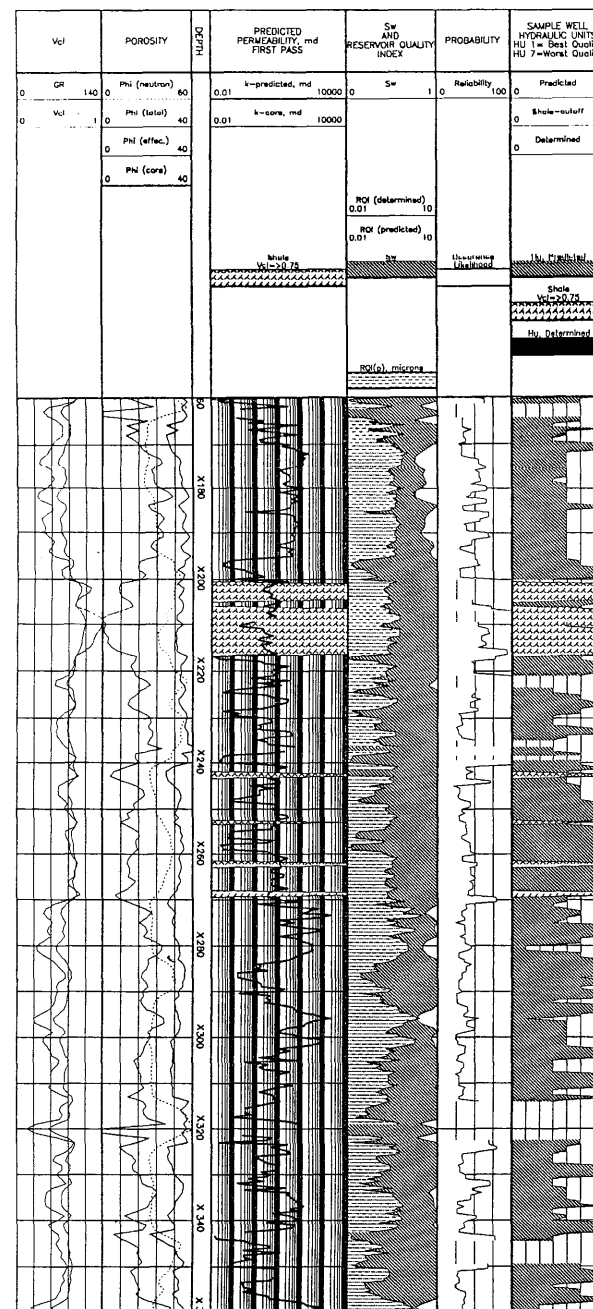

Fig. 28.   Comparison of predicted versus actual permeability from
            k-φ correlation and from hydraulic unit wireline data
            (Far Eastern example).

Fig. 29.   Permeability profile predicted from logging in an
            uncored well (Far Eastern example).